Trilateral Predictor-mediated Teleoperation of a Wheeled Mobile Robot with Slippage

Weihua Li, Haibo Gao, Liang Ding and Mahdi Tavakoli, *Member, IEEE*

Abstract—**With the widespread use of wheeled mobile robots (WMR) in various applications, new challenges have emerged in terms of designing its teleoperation system. One of such challenges is caused by wheel slippage and another is due to the strict need for ensuring WMR safety. This paper proposes a new trilateral teleoperation scheme for haptic teleoperation control of a WMR (slave) with longitudinal slippage. In this teleoperation system, a virtual model (predictor) of the slave WMR is utilized at the master site to guide the human operator to issue more effective commands and, by mediating between the master and the slave WMR, ensure that unsafe maneuvers are not performed by the WMR. Besides compensation for the WMR/terrain's nonpassivity caused by the slippage, a shared control is proposed for the system. Theoretically, the system's stability is shown via its passivity and it is shown that the force felt by the human operator is approximately equal to the forces applied by the environment of the predictor plus that of the slave robot, which is a satisfactory performance outcome. Experiments of the proposed WMR teleoperation system demonstrate that it results in stable trilateral teleoperation with a satisfactory tracking performance. The predictor at the master site is shown to compensate for lack of precise information about the slave robot.**

I. INTRODUCTION

W HEN a wheeled mobile robot (WMR) is travelling on a slippery surface, the ideal assumption of pure rolling is not held any more, which will bring new problems for its control. The slippage phenomenon causes a velocity loss for the WMR relative to a desired input velocity signal [1-5]. With the introduction of slippage, the WMR's kinematic and dynamic models are affected, creating new challenges for its control.

In teleoperation of a WMR, appropriately providing haptic feedback can enhance task performance. For haptic teleoperation of a WMR, there are two kinematics-related challenges not often experienced during teleoperation of non-mobile robots [6]: 1) the workspace of the master robot

W. Li, H. Gao and L. Ding are with the State Key Laboratory of Robotics and System, Harbin Institute of Technology, Harbin, 150001 China. (e-mails: liweihua.08301@163.com, {gaohaibo, liangding}@hit.edu.cn)

W. Li and M. Tavakoli (senior author) is with the Department of Electrical and Computer Engineering, University of Alberta, Edmonton, Alberta, T6G 2V4 Canada (e-mail: mahdi.tavakoli@ualberta.ca). (All correspondence should be addressed to: L. Ding and M. Tavakoli)

is limited, but that of the slave mobile robot is often not or is much bigger, and 2) the wheeled mobile robot is under non-holonomic constraints so that the directions of permissible motions are restricted. Owing to WMR's unlimited workspace, the coordination of master's position (q_m) and slave's velocity (v_s) is commonly considered [6-11]. In [12], the authors also proposed a trilateral two-master/one-slave control approach is proposed for delay-free applications in which the first master controls a primary task control frame, and another master device can manipulate a secondary task frame attached to the slave robot. While past researches are based on the ideal assumption of pure rolling (zero slippage), we will consider the problem of workspace mismatch and surface slippage at the same time.

In WMR teleoperation, since feedback data is limited including the video feedback from the slave robot, the human operator does not know the WMR's detailed states and therefore cannot give effective commands [13, 14]. In some cases, the WMR's safety is the most important performance metric (e.g., in lunar/Mars exploration) [15], thus we need to validate the human commands in advance to guarantee the WMR's safety. Additionally, in the WMR teleoperation scheme, since a coordination of the master robot position and the WMR velocity is enforced to address the workspace mismatch problem mentioned before, the human operator is unable to judge the WMR's accurate position. Smith predictor and Bayesian predictions have been adopted by many researchers to compensate for the delayed or unknown information in the WMR teleoperation scheme [13, 15]. Since the WMR/terrain's interaction is a highly complicated model on loose soil (not pure rolling), the authors have developed a WMR prediction system called ROSTDyn (ROver Simulation based on Terramechanics and Dynamics) [16]. In this paper, we propose a trilateral teleoperation scheme, which inserts a predictor of the slave robot into a WMR bilateral teleoperation loop at the master site. With the help of the predictor, the human operator can operate the slave robot more effectively.

The main contributions of this paper include the following. 1) We present that owing to the WMR/terrain slippage fluctuations, the WMR/terrain's interaction may show nonpassivity, and propose a method to compensate for it while designing the control system, and 2) we propose a WMR trilateral teleoperation scheme coupled with two nonpassive environments, give its stability conditions and analyze its force tracking performance.

The rest of this paper is organized as follows: In Sec. II, the WMR trilateral teleoperation scheme is proposed. In Sec. III,

the WMR's kinematic model with longitudinal slippage is proposed. In Sec. IV, the dynamic/kinematic models for the master/slave are introduced in detail, and the magnitude of the SOP for the environment termination is analyzed. In Sec. V, a WMR trilateral teleoperation system is proposed, and its stability conditions are obtained. In Sec. VI, experiments of the proposed controllers are done to demonstrate the proposed method is effective.

II. WMR TRILATERAL TELEOPERATION SCHEME

In WMR-based bilateral teleoperation system, there are several limitations that need to be considered:

(1) Owing to the WMR's unlimited workspace, a position (master robot)-velocity (slave robot) mapping is often used. In this case, if visual information from the WMR side is not fed back to the operator or its quality is degraded, it will be hard for the human operator to assess the WMR's position.

(2) On surfaces that involve slippage, the WMR's status information not only includes its position/velocity but also its slippage and sinkage, which effects the WMR's safety (e.g., the WMR may be trapped in areas with high slippage and sinkage). This information is much harder to access and evaluate by the operator than the position/velocity information.

(3) In a teleoperation task, having global information about the environment rather than local information is more helpful to give more effective commands.

Therefore, when the visual feedback from the slave WMR is lacking, unreliable or of low quality, or when there is a big time delay in the visual feedback information (e.g., for the lunar rover exploration, the round-trip time delay is about 3-10s), having a predictor of the slave robot including its environment become more valuable. In this paper, based on the WMR bilateral teleoperation architecture [21], a WMR robot's predictor is added to a regular bilateral teleoperation system, and therefore a trilateral teleoperation architecture is proposed.

In our WMR trilateral teleoperation scheme, we insert a simulation-based predictor of the slave robot into a general WMR bilateral teleoperation system as Fig. 1 shows，where r_m is defined later. In this system, the predictor can immediately give a direct sense of the WMR's response to the operator's commands using which the operator can regulate his/her commands effectively. While the master robot interacts with the human operator, the predictor and the slave robot both act like two slave robots, each interacting with its own environment.

In this scheme, through the sharing weights α ($0 < \alpha \leq 1$) shown in Fig. 1, the three robots are coupled with each other to implement an effective prediction of the slave robot. Choosing the sharing parameter in a real scenario depends on the predictor's fidelity: if the predictor makes highly accurate predictions, α can be set as 1, in which case the predictor is only commanded by the human operator and provides an ideal prediction of the slave robot's behavior. If there are prediction errors between the predictor and the slave robot, we should decrease α to make the slave robot take a role in the control of the predictor and implement a good velocity

prediction; however, we should avoid α=0, in which case, the predictor will lose its prediction function.
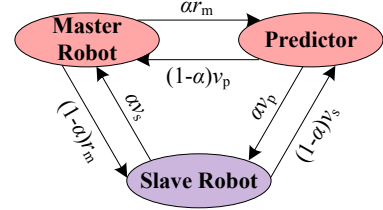

Figure 1. WMR trilateral sharing control.

III. WMR'S KINEMATIC MODEL SUBJECT TO SLIPPAGE

In this paper, a two-wheel actuated mobile robot is considered as Fig. 2(a) shows. The two back wheels are the driving wheels and the front wheel is free moving. However, here we assume that this WMR only travels forward or backward without any rotation and, therefore, is free from non-holonomic constraints. In the ideal case of wheel's pure rolling, the wheel's linear velocity v will be equal to its angular velocity ω multiplied by the wheel's radius r. As seen in Fig. 2(b), an angular velocity-level controller is embedded in the WMR. Ideally, it can be assumed that the transfer function from ω_d to ω is unity. Therefore, the WMR's kinematic model incorporating the embedded angular velocity controller can be described as

$$v = v_{d} , \qquad (1)$$

where $v_{d} = r\omega_{d}$.

However, when the WMR is traveling on a soft terrain such as sand or loose soil, due to the limited driving forces and possible opposing external forces, the WMR's linear velocity v will no longer be equal to the wheel's angular velocity ω times r. Instead, longitudinal slippage S will happen at the contact-area between the wheel and the terrain, which can be defined as [5]:

$$S = \begin{cases} (r\omega - v)/v & (\omega \neq 0) \\ 0 & (\omega = 0) \end{cases} . \qquad (2)$$

The above relationship has been modeled by the feedback loop in Fig. 2(b).

In the ideal case that $\omega_{d} = \omega$, we have $r\omega = v_{d}$ and (2) can be expressed as $S = (v_{d} - v)/v$. Let us define δ as

$$\delta = v_{d} - v , \qquad (3)$$

where δ is the velocity loss caused by wheel's slippage. Based on (2), we know that $\delta = Sv$.

Evidently, in the presence of slippage, the embedded angular velocity controller cannot result in good linear velocity tracking any more. Therefore, an *embedded angular acceleration-level* controller is considered which works based on the difference of the WMR's desired velocity and its actual velocity as shown in Fig. 2(c). We also assume a unity transfer function from $\dot{\omega}_d$ to $\dot{\omega}$. The WMR model relating the wheel's angular acceleration and the WMR's linear acceleration in the presence of slippage is found next. By differentiating $Sv = r\omega - v$ obtained from (2), we can get

$$r\left(\dot{\omega} - \underbrace{\frac{1}{r}\left(S\dot{v} + \dot{S}v\right)}_{\text{slippage model}}\right) = \dot{v} . \qquad (4)$$

Here, S and $\dot{S}$ are both time-varying parameters.

In Fig. 2(c), a_d is the desired linear acceleration for the WMR based on the linear velocity difference, which is then passed to the angular acceleration-level controller embedded in the WMR. Since in Fig. 2(c), the transfer function from $\dot{\omega}_d$ to $\dot{\omega}$ is assumed to be unity, Fig. 2(c) can be simplified as Fig. 2(d).
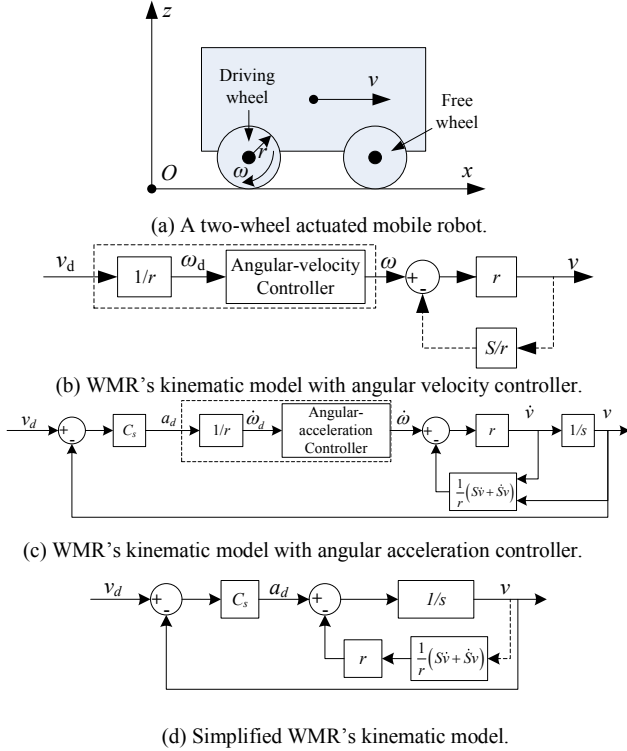

(a) A two-wheel actuated mobile robot.

(b) WMR's kinematic model with angular velocity controller.

(c) WMR's kinematic model with angular acceleration controller.

(d) Simplified WMR's kinematic model.

Figure 2.   WMR's kinematic model and control.

IV.   SLAVE/MASTER ROBOT MODEL

A. Slave Robot's Model

With the WMR acting as the slave robot of the teleoperation system, we are interested in modeling the terrain-dependent longitudinal slippage caused by the interaction between the wheel and terrain as the "environment termination" (ET) with which the slave robot interacts. From (3) and $\delta = Sv$, we get

$$\dot{\delta}(t) = S(t)\dot{v}(t) + \dot{S}(t)v(t). \qquad (5)$$

From the definition of the slippage in (2), slippage looks to be a function of the wheel linear velocity and wheel angular velocity. However, in practice, the slippage is not decided by these, but by the WMR/terrain contact characteristics. Therefore, $\dot{\delta}(t)$ in (5) can be seen as the contribution of the external environment (terrain) to decide the WMR's linear acceleration where there is longitudinal slippage.

In this paper, the case of $r\omega > v$ is considered, which corresponds to $s > 0$, implying that the wheel slippage causes a *reduction* in the linear velocity of the WMR. Meanwhile, it is assumed that the rate of change of slippage is constrained by $\dot{S}_L < \dot{S} < \dot{S}_U$ where $\dot{S}_L$ and $\dot{S}_U$ are decided by the WMR's states and the terrain's parameters.

Defining the control input $u_s = a_d$ and the environment interaction force δ_e, the kinematic model of the slave robot can be found based on (4) and (5) as

$$\dot{v}_s = u_s - \delta_e , \qquad (6)$$

where $\delta_e(t) = S(t)\dot{v}_s(t) + \dot{S}(t)v_s(t)$.

The above equation provides a straightforward model of the WMR as a slave robot in an interaction with the terrain. In the above, the environment interaction force δ_e represents a generalization of the terrain-dependent slippage-induced force.

The following property is proposed to determine the passivity or non-passivity of the system (5).

Property 1 The LTV (Linear Time-Invariant) system (5), when $\dot{S}$ is negative, is input non-passive (INP) with a shortage of passivity (SOP) of $-0.5\dot{S}_L$.

Proof: With the input $v_s(t)$ and output $\delta_e(t)$, the system (5) satisfies the following inequality for all $v_s(t)$ and $T \geq 0$:

$$\int_0^T \delta_e(t)v_s(t)dt = \int_0^T v_s(t)\left(S(t)\dot{v}_s(t) + \dot{S}(t)v_s(t)\right)dt$$

$$= \underbrace{V(T) - V(0)}_{Z_{e1}} + \frac{1}{2}\underbrace{\int_0^T \dot{S}(t)v_s(t)v_s(t)dt}_{Z_{e2}} , \qquad (7)$$

$$\geq -V(0) + \frac{1}{2}\dot{S}_L\underbrace{\int_0^T v_s(t)v_s(t)dt}_{Z_{e2}}$$

where $V(t) = \frac{1}{2}S(t)v_s^2(t) \geq 0$ since it was assumed that $S(t) \geq 0$. As shown above, the input-output passivity integral [17] is decomposed into two parts: a passive part (Z_{e1}) and a potentially active part (Z_{e2}). When $\dot{S}$ is positive, the system will dissipate energy and cause an excess of passivity, so it is strictly passive. However, when $\dot{S}$ is negative, as (7) shows, this system may accumulate energy and become INP with the largest (worst-case) SOP of $-0.5\dot{S}_L$. Therefore, the ET (5) can be an INP system with a SOP of $-0.5\dot{S}_L$.

B. Master robot's model

For a single-joint master robot, its dynamics can be written as

$$M_m\ddot{q}_m + B_m\dot{q}_m = \tau_m + \tau_h , \qquad (8)$$

where, M_m and B_m are the master robot's mass and damping coefficient, q_m is the degree of freedom, τ_m and τ_h are the forces/torques applied by the motor and human operator.

In general non-mobile robot teleoperation systems, the master and slave velocities (and positions) are synchronized. However, due to the unlimited workspace of the WMR, the coordination between the master's position q_m and the slave's velocity v_s is more appropriate and utilized. Inspired by [6], a new variable $r_m = \lambda \dot{q}_m + q_m$ where $0 < \lambda < 1$ is used instead of $\dot{q}_m$ in the coordination; then, the problem will require coordinating r_m and v_s. When λ and/or $\dot{q}_m$ is small, an approximate coordination of position-velocity ($q_m \approx v_s$) can be achieved between the master robot and the slave mobile robot.

The controller τ_m in (8) is designed as $\tau_m = \tau_m^* + \bar{\tau}_m$, with a local controller τ_m^* and a term $\bar{\tau}_m$ that will be designed in Sec. V. In terms of the new variable r_m and with the local controller $\tau_m^* = -B_{Lv}\dot{q}_m - B_{Lp}q_m$, the master robot's dynamic model (8) can be rewritten as

$$\bar{M}_m \dot{r}_m + \bar{B}_m r_m = \bar{\tau}_m + \tau_h, \qquad (9)$$

where $\bar{M}_m = M_m/\lambda$, $\bar{B}_m = B_{Lp}$ and $B_{Lv} = \dfrac{M_m}{\lambda} + \lambda B_{Lp} - B_m$.

As [6] presented, we also assume the human operator can adjust his/her impedance to ensure the passivity of its impedance when augmented with the position/velocity mapping. This assumption is seen in an overwhelming majority of the teleoperation literature [18].

V. WMR TRILATERAL TELEOPERATION SYSTEM DESIGN

A. Controller design

Based on the above analysis, we propose a new WMR trilateral teleoperation scheme as Fig. 3 shows. The predictor at the master site cannot directly initiate any new command to the slave WMR in the way that the human operator does but it can affect the human's commands. In Fig. 3, MCU encompasses the master and its controller and SCU consists of the slave and its controller. HT is the human termination, ET_P and ET_S is the environment termination (ET) of the predictor and slave robot, and CC is the communication channel.
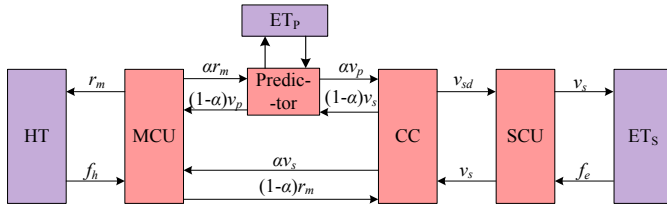

Figure 3.   WMR Trilateral teleoperation scheme.

Since the predictor is a dynamic prediction of the slave robot, their models are similar (in the experiments, we consider the case where the slave robot and the predictor do not have the exact same model). Therefore, in the WMR trilateral teleoperation system, each robot's dynamic/kinematic model is as follows:

$$\begin{cases} \text{Master: } \bar{M}_m \dot{r}_m = \tau_m + \tau_h \\ \text{Predictor: } \dot{v}_p = u_p - \delta_p \\ \text{Slave: } \dot{v}_s = u_s - \delta_s \end{cases} \qquad (10)$$

where the predictor and the slave robot's model in this equation is same with (6).

By using the shared control scheme in Fig. 1, we design the controllers for the master robot, the predictor, and the slave robot as:

$$\begin{cases} \text{Master: } \tau_m = C_m \left(\alpha v_s + (1-\alpha) v_p - r_m \right) \\ \text{Predictor: } u_p = C_p \left(\alpha r_m + (1-\alpha) v_s - v_p \right) - K_p v_p \\ \text{Slave: } u_s = C_s \left(\alpha v_p + (1-\alpha) r_m - v_s \right) - K_s v_s \end{cases} \qquad (11)$$

The position/velocities of the master robot, the predictor and the slave robot can track each other, which can be seen in Sec. V. Also, the damping elements in these controllers are used to modify the nonpassivity of the ET. Based on the analysis in Sec. III, we can estimate the SOP of ET by (7), and then use the damping elements to compensate for it. Therefore, $K_p - \varepsilon_p = 0$, $K_s - \varepsilon_s = 0$.

Therefore, based on (10) and (11), we can obtain this system's impedance matrix Z as:

$$\begin{bmatrix} \tau_h \\ \delta_p \\ \delta_s \end{bmatrix} = \underbrace{\begin{bmatrix} M_m s + C_m & (1-\alpha) C_m & \alpha C_m \\ \alpha C_p & s + C_p & -(1-\alpha) C_p \\ (1-\alpha) C_s & -\alpha C_s & s + C_s \end{bmatrix}}_{Z} \begin{bmatrix} r_m \\ -v_p \\ -v_s \end{bmatrix}. (12)$$

In practice, since the models of the predictor and the slave robot are similar, it makes sense that the controller parameters are assumed as

$$C_m = \beta C_s = \beta C_p, \qquad (13)$$

where β is an amplification coefficient.

Lemma 1 [19] The necessary and sufficient conditions for passivity of a 3-port network (12) are

1) The z-parameters (elements of the impedance matrix Z) have no RHP poles.

2) Any poles of the z-parameters on the imaginary axis are simple, and the residues k_{ij} of z-parameters at these poles satisfy the following conditions:

(1) $k_{ii} \geq 0 \qquad i = 1, 2, 3$;

(2) $\dfrac{k_{11}k_{22} - k_{21}k_{12}}{k_{11}} \geq 0$;

(3) $\dfrac{k_{11}k_{33} - k_{31}k_{13}}{k_{11}} - \dfrac{(k_{11}k_{23} - k_{21}k_{13})(k_{11}k_{32} - k_{31}k_{12})}{k_{11}(k_{11}k_{22} - k_{21}k_{12})} \geq 0$.

3) The complex z'-parameters satisfy the following conditions for all real frequencies ω:

(1) $z_{ii}' \geq 0 \qquad i = 1, 2, 3$;

(2) $\dfrac{z_{11}'z_{22}' - z_{21}'z_{12}'}{z_{11}'} \geq 0$;

(3) $\dfrac{z_{11}'z_{33}' - z_{31}'z_{13}'}{z_{11}'} - \dfrac{(z_{11}'z_{23}' - z_{21}'z_{13}')(z_{11}'z_{32}' - z_{31}'z_{12}')}{z_{11}'(z_{11}'z_{22}' - z_{21}'z_{12}')} \geq 0$,

where $z_{ij}' = \dfrac{1}{2}\left(z_{ij} + z_{ji}^*\right)$.

Based on Lemma 2, we can obtain the absolute stability conditions for the system (12) as:

(1) $C_m, C_p, C_s \geq 0$;

(2) $\dfrac{C_m C_p - \alpha (1-\alpha) C_m C_p}{C_m} \geq 0$;

(3) $\dfrac{C_m C_s - \alpha (1-\alpha) C_m C_s}{C_m} -$
$\dfrac{\left[(1-\alpha) C_m C_p + \alpha^2 C_m C_p\right]\left[\alpha C_m C_s + (1-\alpha)^2 C_m C_s\right]}{C_m \left(C_m C_p - \alpha(1-\alpha) C_m C_p\right)} \geq 0$.

By simplifying these conditions, we can get the following absolute stability conditions for any frequency ω and any sharing weight parameter α ($0 < \alpha \leq 1$):

$$C_m, C_p, C_s \geq 0. \tag{14}$$

B. Force transparency

Based on the system's impedance matrix (12), we can derive its hybrid matrix as

$$\begin{bmatrix} \tau_h \\ -v_p \\ -v_s \end{bmatrix} = \begin{bmatrix} h_{11} & h_{12} & h_{13} \\ h_{21} & h_{22} & h_{23} \\ h_{31} & h_{32} & h_{33} \end{bmatrix} \begin{bmatrix} r_m \\ \delta_p \\ \delta_s \end{bmatrix}, \tag{15}$$

where,

$h_{11} = M_m s + C_m + \Delta$

$\Delta = \dfrac{-\left[\alpha s C_p + (1-\alpha+\alpha^2) C_p C_s\right](1-\alpha) C_m}{(s+C_p)(s+C_s) - (1-\alpha)\alpha C_s C_p} +$
$\dfrac{-\left[(1-\alpha) s C_s + (1-\alpha+\alpha^2) C_p C_s\right]\alpha C_m}{(s+C_p)(s+C_s) - (1-\alpha)\alpha C_s C_p}$

$h_{12} = \dfrac{(1-\alpha) C_m (s+C_s) + \alpha C_m \alpha C_s}{(s+C_p)(s+C_s) - (1-\alpha)\alpha C_s C_p}$

$h_{13} = \dfrac{(1-\alpha)^2 C_m C_p + \alpha C_m (s+C_p)}{(s+C_p)(s+C_s) - (1-\alpha)\alpha C_s C_p}$

Based on this H-matrix (15), we can obtain the force felt by the human operator as

$$\tau_h = h_{11} r_m + h_{12} \delta_p + h_{13} \delta_s. \tag{16}$$

Assuming the system is stable and at the steady-state, which means $\omega \to 0$, we can ignore the system's high-order elements. Then, the elements of (16) will become

$h_{11} \approx C_m + \dfrac{-\left[(1-\alpha+\alpha^2) C_s^2\right]\left[(1-\alpha) C_m + \alpha C_m\right]}{(1-\alpha+\alpha^2) C_s^2}$

$\approx 0 \, (s \to 0)$

$h_{12} = \dfrac{(1-\alpha) C_m (s+C_s) + \alpha C_m \alpha C_s}{(s+C_p)(s+C_s) - (1-\alpha)\alpha C_s C_p}$

$\approx \beta \, (s \to 0)$

$h_{13} = \dfrac{(1-\alpha)^2 C_m C_p + \alpha C_m (s+C_p)}{(s+C_p)(s+C_s) - (1-\alpha)\alpha C_s C_p}$

$\approx \beta \, (s \to 0)$

Therefore, while the system is stable, the force felt by the human operator is

$$\tau_h \approx \beta \delta_p + \beta \delta_s. \tag{17}$$

This equation shows that the human operator feel both the predictor's environment force and the slave robot's environment force at the same time. Thus, the system's force transparency is good.

VI. EXPERIMENTS

In the case studies below, the trilateral teleoperation of a mobile robot in an environment with slippage is considered. It is known that the slippage varies with the soil's mechanical parameters (e.g., friction angle) [15] and the terrain's parameters (e.g., slope angle). Limited by implementation issues concerning recreating specific terrain characteristics that give rise to certain shortage of passivity of the environment model, we perform semi-physical experiments to validate the proposed WMR trilateral teleoperation scheme under longitudinal slippage.

A. Experiments setup

To validate the proposed scheme, experiments are done using a Phantom Premium 1.5A haptic device (master robot) and two ROSTDyn (one is used as predictor; the other is used as slave robot). The experimental system is detailed below.

(1) Master robot and human operator

In our WMR's trilateral teleoperation system, the master robot is a Phantom Premium 1.5A haptic device (Geomagic Inc., Wilmington, MA, USA), and the predictor and the slave robot (WMR) is a WMR's simulation platform called ROSTDyn which has been developed by the authors [16], and the communication in them is implemented using local area network (LAN). Considering just one degree of freedom (DOF) motion, the first joint q_1 of the Phantom is used and the other two joints are locked by a high gain position controller ($q_2 = q_3 = 0$). Based on the research results from [20], the Phantom's inertia is $M_m = 0.0035$. In (9), λ=0.1 and $B_{Lv} = -0.035$.

In the experiments, based on (9), the force applied on the master robot by human operator is estimated as

$$\tau_h = \bar{M}_m \dot{r}_m + \bar{B}_m r_m - \bar{\tau}_m. \tag{18}$$

(2) Slave robot and environment

In our WMR's trilateral teleoperation system, ROSTDyn is used as the slave robot and developed based on Vortex software (CMLabs, Montreal, Canada) and the simplified terramechanics model. ROSTDyn can realize a real-time simulation with a good fidelity [16]. In this paper, we separately use two ROSTDyn instances to simulate a WMR moving on a soft terrain, which causes slippage (one is the

predictor and the other is the slave robot). The following is the terramechanics model between the wheel and terrain in ROSTDyn:

$$\begin{cases} F_{\mathrm{N}} = rb\sigma_m A + rb\tau_m B = AX + BY \\ F_{\mathrm{DP}} = rb\tau_m A - rb\sigma_m B = AY - BX \;, \\ M_{\mathrm{R}} = r^2 b(\theta_1 - \theta_2)\tau_m /2 = rCY \end{cases} \quad (19)$$

where $A = \dfrac{\cos\theta_m - \cos\theta_2}{\theta_m - \theta_2} + \dfrac{\cos\theta_m - \cos\theta_1}{\theta_1 - \theta_m}$;

$B = \dfrac{\sin\theta_m - \sin\theta_2}{\theta_m - \theta_2} + \dfrac{\sin\theta_m - \sin\theta_1}{\theta_1 - \theta_m}$; $C = (\theta_1 - \theta_2)/2$;

$X = rb\sigma_m$; $Y = rb\tau_m$; $\tau_m = E(c + \sigma_m \tan\varphi)$;

$\sigma_m = K_s r^N (\cos\theta_m - \cos\theta_1)^N$; $K_S = K_c/b + K_\varphi$; $N = n_0 + n_1 s$;

$E = 1 - \exp\{-r[(\theta_1 - \theta_m) - (1 - s)(\sin\theta_1 - \sin\theta_m)]/K\}$.

In (19), F_N is the normal force, F_{DP} is the drawbar pull force, and M_R is the moment generated by the interaction between the wheel and the terrain, s is the slippage of a wheel and φ is the internal friction angle. The other parameters are defined in [16]. This model mainly connects the WMR's dynamics and wheel's sinkage and slippage. For the normal force F_N, its magnitude is mostly decided by the wheel's sinkage. The softer the terrain is (corresponding to the parameter K_s), the bigger the sinkage is. Similarly, if the load in the moving direction increases, the required drawbar pull force will increase, and as a result, the wheel's slippage increases.

The predictor and the slave robot use the same terrain. This terrain has a slope with an angle of 15°, and its size is 10m (x)×10m (y). Since we are focusing on creating a nonpassive ET caused by the slippage, and the slippage model cannot be directly given, the most sensitive parameter to the slippage, which is φ in (19), is considered and set as a terrain-varying function. In practice, φ is decided by the soil's characteristics. However, the predictor always has a model error (mainly slippage error) compared with the real WMR. In this paper, we accumulated these errors on the parameter φ to validate the proposed method. Therefore, in the predictor and slave robot, the values of φ are different. The following model makes the terrain become harder as the WMR travels forward:

$$\varphi_p = \begin{cases} 1.35 & (8.1 \le x < 10) \\ 0.6 + 0.15(x - 3.1) & (3.1 \le x < 8.1) \;. \\ 0.6 & (0 < x < 3.1) \end{cases} \quad (20)$$

$$\varphi_s = \begin{cases} 1.3 & (6.6 \le x < 10) \\ 0.6 + 0.2(x - 3.1) & (3.1 \le x < 6.6) \;. \\ 0.6 & (0 < x < 3.1) \end{cases} \quad (21)$$

Here, x is the WMR position along the moving direction. In the case of climbing a sloped terrain, the bigger the φ, the smaller the slippage, which will cause a negative $\dot{s}$ while S is positive, which causes the ET's potential nonpassivity.

In the following experiments, the master robot provides r_m, which acts as a reference value for to the predictor and slave robot's velocity. Owing to the time-varying slippage, the actual slave robot's velocity v_s/v_p may be different from this

commanded velocity and a velocity-error is caused, the human operator will feel these differences through the feedback command velocity to the master. If r_m is bigger than the required velocity, a backward force will be felt by the human operator that pushes back on the master robot; if r_m is smaller than the required velocity, a forward force will be felt by the human operator that pulls the master robot forward. Therefore, in this teleoperation scheme, force feedback guides the human operator to give a more effective command to the slave WMR.
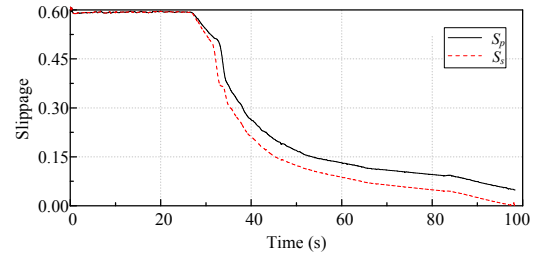
B. Experimental results

To validate the proposed WMR trilateral teleoperation scheme, the following experiments are done with different controller parameters:

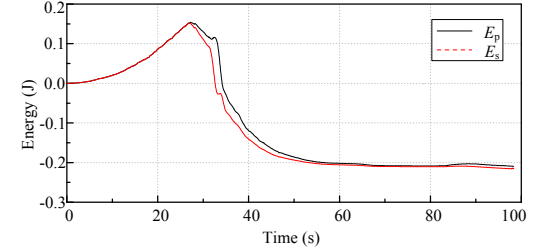Case I: $C_m = C_s = C_p = 15$, $\alpha = 0.5$ and $K_s = 0$;

Case II: $C_m = C_s = C_p = 15$, $\alpha = 0.5$ and $K_s = 0.8$;

Case III: $C_m = C_s = C_p = 10$, $\alpha = 1.0$ and $K_s = 0$;

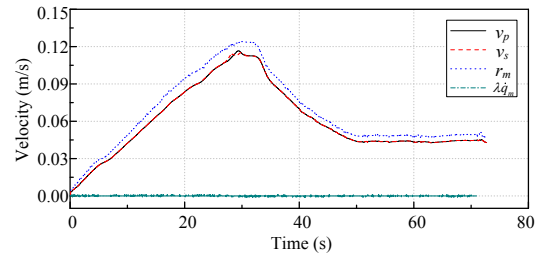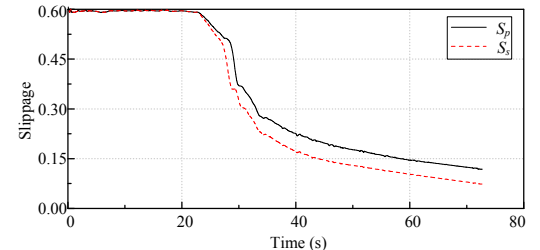Case IV: $C_m = C_s = C_p = 10$, $\alpha = 1.0$ and $K_s = 0.8$;

(a) Slippage curve.

(b) ET's energy curve.

Figure 4.   Experimental results with Case I.

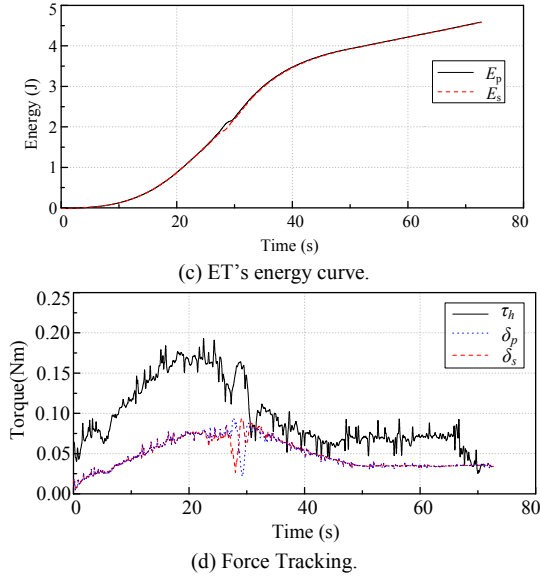(a) Position-velocity coordination.

(b) Slippage curve.

(c) ET's energy curve.

(d) Force Tracking.

Figure 5.   Experimental results with Case II.

(a) Slippage curve.

(b) ET's energy curve.
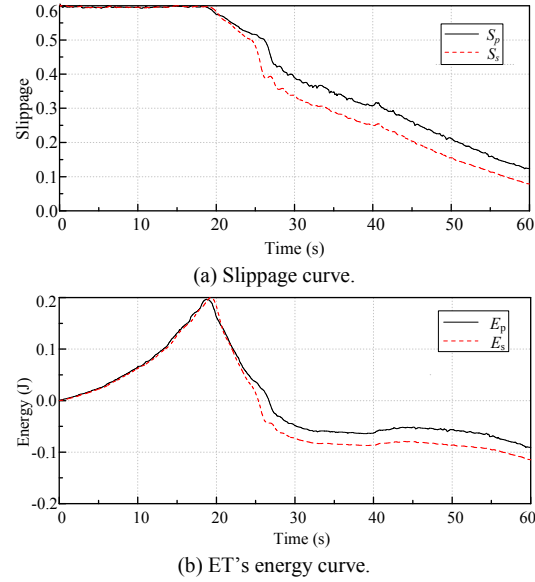
Figure 6.   Experimental results with Case III.

(a) Position-velocity coordination.

(b) Slippage curve.
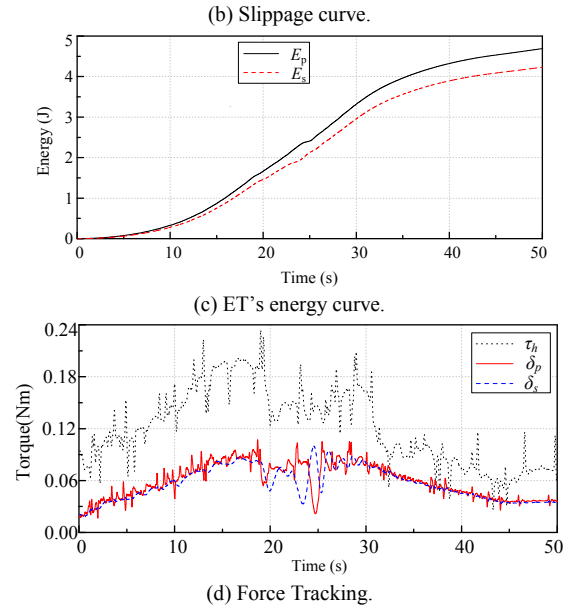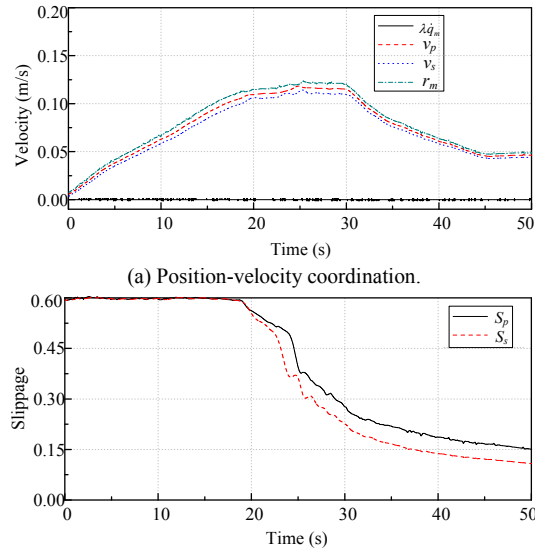

(c) ET's energy curve.

(d) Force Tracking.

Figure 7.   Experimental results with Case IV.

From the experimental results of Fig. 4 – Fig. 7, we can obtain the following colusions :

(1) Under the given terrain parameters, the WMR/terrain environment including the predictor and the slave robot is a nonpassive system (Fig. 4(b) and Fig. 6(b)) owing to the time-decreasing slippage (Fig. 4(a) and Fig. 6(a)).

(2) Since the ET (including ET_P and ET_S) is nonpassive, without the SOP compensation, the system is potentially unstable (Case I, III).

(3) By utilizing the proposed SOP compensation by K_p and K_s, ε_s and ε_p is decided by the slippage curve (Fig. 5 (b) and Fig. 7 (b)) and it makes sense that it is equal to 0.8. The modified ET becomes passive (Fig. 5 (c) and Fig. 7 (c)) and presents a damping characteristic to some extent.

(4) With the modified passive ET, the system is stable (Fig. 5 (a) and Fig. 7 (a)), and the human operator feels like interacting with a damping (Fig. 5 (d) and Fig. 7 (d)).

(5) The system's force tracking performance (Fig. 5 (d) and Fig. 7 (d)) is weakly influenced by the sharing weight α. From the results, we can see that the human force is almost equal to δ_p plus δ_s, as the theory predicts in (17) (here, β=1).

(6) Owing to the modified ET's damping characteristic, the system's position-velocity tracking performance is influenced by the SOP compensation, and this coordination is further influenced by the sharing weight α. Particularly, the velocity-tracking performance between the predictor and the slave robot in Case II (α=0.5) is better than that in Case IV (α=1.0) as the analysis in Sec. II.

(7) The good position-velocity tracking and force tracking performance validate that the predictor at the master site can be used to compensate for the unknown information of the slave robot, and is helpful for the human operator to give more effective commands.

Additionally, to validate the proposed trilateral teleoperation scheme, a comparison experiment between the WMR bilateral teleoperation scheme in [21] and the WMR trilateral teleoperation scheme proposed here is done. In this experiment, the controller parameters are designed to make

each scheme stable. The human operator teleoperates the WMR to arrive at a given position (1.8m) and avoid the potential obstacles in the travel. The experimental results are shown in Table 1.

TABLE 1 Comparision between WMR bilateral teleoperation and trilateral scheme in this paper.

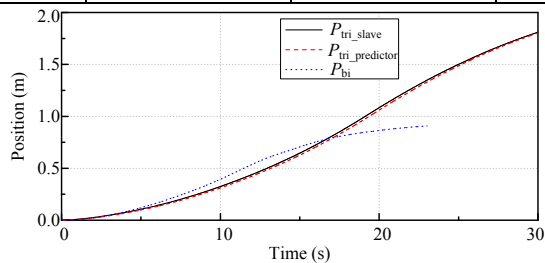| Scheme	Status feedback of WMR	Environment feedback	Task completion
Bilateral Scheme [21]	Part(velocity)	Part(Environment force caused by slippage)	NO
Trilateral scheme in this paper	WMR's position, slippage, sinkage etc.	Whole environment around WMR	Yes

Figure 8.   Task performance comparison between WMR bilateral scheme and trilateral scheme in this paper.

From the experimental results, we can see that if the WMR-side video information is unavailable to the operator, through the predictor, the operator can still feel or see the WMR's position, slippage, sinkage and other states information, which can help the human to estimate the WMR's performance and safety. Meanwhile, the human operator can sense the surrounding environment even if there is no feedback force resulting from hitting obstacles. Therefore, with the help of the predictor, the human operator can implement a more accurate task under the position-velocity mapping and guarantee the WMR's safety with the help of the predictor as Fig. 8 shows.

VII. CONCLUSION

A new trilateral teleoperation scheme for haptic teleoperation control of a WMR with longitudinal slippage is proposed in this paper. In this teleoperation system, the mobile robot's linear velocity follows the master haptic interface's position, and the predictor is used as a prediction of the slave robot. The nonpassivity of the environment terminations for the predictor (ET_P) and the slave robot (ET_S) are separately compensated for by two damping controllers. The system's stability conditions are given by guaranteeing its passivity. Theoretical analysis shows the force felt by the human operator is almost equal to the force applied by the predictor's environment termination (δ_p) plus that for the slave robot (δ_s). Experiments of the system demonstrate the validity of the proposed WMR trilateral teleoperation system. In the future, the WMR's rotation motion and teleoperation communication channel delays will be further considered in the stability analysis and control design.

REFERENCE

[1] L. Ding, H. Gao, Z. Deng, K. Yoshida, et al, "Experimental study and analysis on driving wheels' performance for planetary exploration rovers moving in deformable soil," in *J. Terramech.* vol. 48, no. 1, pp. 27–45, 2011.

[2] L. Ding, K. Nagatani, K. Sato, et al, "Terramechanics-based high-fidelity dynamics simulation for wheeled mobile robot on deformable rough terrain," in *Proc. IEEE Int. Conf. Robot. Autom.*, Anchorage, 2010, pp. 4922–4927.

[3] Giulio Reina, Lauro Ojeda, Annalisa Milella, and Johann Borenstein, "Wheel Slippage and Sinkage Detection for Planetary Rovers," in *IEEE Transactions on Robotics*, vol. 11, no. 2, pp. 185-195, 2011.

[4] G. Ishigami, K. Nagatani, and K. Yoshida, "Path Following Control with Slip Compensation on Loose Soil for Exploration Rover," in *Proc. IEEE/RSJ Int. Conf. Intell. Robots Syst.*, Beijing, 2006, pp. 5552-5557.

[5] Yu Tian , Nilanjan Sarkar, "Control of a Mobile Robot Subject toWheel Slip" in *J Intell Robot Syst*, vol. 74, no. 4, pp. 915-929, 2014.

[6] Dongjun Lee, Oscar Martinez-Palafox, and Mark W. Spong, "Bilateral Teleoperation of a Wheeled Mobile Robot over Delayed Communication Network," in *Proc. IEEE Int. Conf. Robot. Autom.*, Orlando, 2006, pp. 3298-3303.

[7] Ildar Farkhatdinov and Jee-Hwan Ryu, "Improving Mobile Robot Bilateral Teleoperation by Introducing Variable Force Feedback Gain," in *Proc. IEEE/RSJ Int. Conf. Intell. Robots Syst.*, Taipei, 2010, pp. 5812-5817.

[8] Farrokh Janabi-Sharifi and Iraj Hassanzadeh, "Experimental Analysis of Mobile-Robot Teleoperation via Shared Impedance Control," *IEEE Trans. Syst. Man Cybern. Part B: Cybern.*, vol. 41, no. 2, pp. 591-606, 2011.

[9] Ha Van Quang, Ildar Farkhatdinov and Jee-Hwan Ryu, "Passivity of Delayed Bilateral Teleoperation of Mobile Robots with Ambiguous Causalities: Time Domain Passivity Approach," in *Proc. IEEE/RSJ Int. Conf. Intell. Robots Syst.*, 2012, pp. 2635-2640.

[10]Pawel Malysz and Shahin Sirouspour, "A Task-space Weighting Matrix Approach to Semi-autonomous Teleoperation Control," in *Proc. IEEE/RSJ Int. Conf. Intell. Robots Syst.*, San Francisco, 2011, pp. 645-652.

[11]Malysz, Pawel, and Shahin Sirouspour. "Task Performance Evaluation of Asymmetric Semiautonomous Teleoperation of Mobile Twin-Arm Robotic Manipulators." *Haptics, IEEE Transactions on*, vol. 6, no. 4, pp. 484-495, 2013.

[12]Malysz, Pawel, and Shahin Sirouspour. "Trilateral teleoperation control of kinematically redundant robotic manipulators." *The International Journal of Robotics Research*, vol. 30, no. 13, pp. 1643-1664, 2011.

[13]Jae-young Lee and Shahram Payandeh, "Stability of Internet-Based Teleoperation Systems Using Bayesian Predictions," in *IEEE World Haptics Conference*, Istanbul, 2011, pp. 499-504.

[14]Shihua Wang, Bugong Xu, Yunyi Jia and Yun-Hui Liu, "Real-Time Mobile Robot Teleoperation over IP Networks Based on Predictive Control," in *IEEE International Conference on Control and Automation*, Guangzhou, 2007, pp. 2091-2096.

[15]The Rover Team, "Characterization of the Martian Surface Deposits by the Mars Pathfinder Rover, Sojourner," *Science*, vol. 278, no. 5344, pp. 1765-1768, 1997.

[16]Weihua Li, Liang Ding, Haibo Gao et al, "ROSTDyn: Rover simulation based on terramechanics and dynamics," *J Terramech*, vol. 50, pp. 199-210, 2013.

[17]Lozano, R., Maschke, B., Brogliato, B. and Egeland, O.: Dissipative systems analysis and control: theory and applications. Secaucus: Springer-Verlag New York, 2007.

[18]Tavakoli, M., Aziminejad, A., Patel, V.R. and Moallem, M., "High-fidelity bilateral teleoperation systems and the effect of multimodal haptics," *IEEE Trans. Syst. Man Cybern. Part B: Cybern.*, vol. 37, no. 6, pp. 1512-1528, 2007.

[19] Victor Mendez, Mahdi Tavakoli and Jian Li, "A Method for Passivity Analysis of Multilateral Haptic Systems," *Advanced Robotics*, vol. 28, no. 18, pp. 1205-1219, 2014.

[20]Cavusoglu, M., C., Feygin, D. and Tendick, F., "A critical study of the mechanical and electrical properties of the PHANToM haptic interface and improvements for high performance control," *Presence: Teleoperators & Virtual Environments*, vol. 11, no. 6, pp. 555-568, 2002.

[21]Li, W., Ding, L., Gao, H. and Tavakoli, M., "Kinematic bilateral teleoperation of wheeled mobile robots subject to longitudinal slippage," *IET Control Theory & Applications*, DOI: 10.1049/iet-cta.2015.0299.